

CHAOTIC BEHAVIOR IN A PLANE PENDULUM WITH A SINUSOIDAL DRIVING TORQUE AT THE PIVOT POINT

COMPUTATIONAL PHYSICS

DEPARTMENT OF PHYSICS

UNIVERSITY OF HONG KONG

TAM HO WON

Introduction of problem

Plane pendulum system consists of a mass m hanging from a specific rigid point restricted in two-dimensional space. Study of pendulum can be retraced to the 16th century that Galileo Galilei studied the physical properties exhibited in chandeliers, then simple iron pendulum.

Chaotic dynamics can be described as nonrandom complicated motions which are perfectly deterministic depending sensitively on the given initial conditions [1]. As a result, a slight change of initial parameters will lead to exponential changes in the final dynamics of the system [2]. Such sensitive dependence on initial conditions results in difficulties predicting motion which makes the system chaotic. This is because no matter how many significant figures one can reassure for the initial conditions, the deviation will be magnified as time passes by and eventually the actual motion is unpredictable. In general, solutions of differential equations describing chaotic dynamics neither converge nor settle into periodic motion. According to the discovery by Lorenz in the 1960s, any uncertainty for initial conditions in the end will result in large error.

Chaos exists across different systems in nature, including weather forecasting, meteorology, [3] Systems which exhibit chaotic behaviors may show similar behaviors during the transition from periodic to chaotic dynamics so it is meaningful for us to investigate the chaotic behaviors. Even though chaotic dynamics may seem to be random and unpredictable, it is deterministic. Yet, nonlinear differential equation is difficult or even impossible to solve analytically implying that the solution may not exist or not always unique even there is a solution. [4]

With the development of computational power and numerical algorithm, it can help to solve the differential equations numerically to simulate the trajectory of chaotic dynamics. This is because usually the chaotic behaviors appear only when large amount of data points was calculated repetitively. In this work, a plane pendulum driven by a sinusoidal driving torque at the pivot point was simulated. Even though for the case of small θ ($<10^\circ$) and no external torque, the motion can be simplified into a simple pendulum, the nonlinear term $\sin\theta$ will become significant as θ increases and transit the system into a chaotic one. To solve the second order nonlinear ordinary differential equations, MATLAB was used to implement numerical methods including Euler's Method and forth order Runge-Kutta method. Two methods were compared in simple harmonic oscillator to determine the accuracy of method with same step size. Through converting the iterative methods into programs, simulation of the motion was done. The features of the motion were observed and discussed.

Physics background

Based on Newton's second law, the equation describing the corresponding motion:

$$I \frac{d^2\theta}{dt^2} + b \frac{d\theta}{dt} + mgl \sin\theta = \tau_{ext}(t) = \tau_0 \sin(\omega_{ext}t) \quad (1)$$

where

l = length between the center of mass and pivot;

m = mass of small mass attached on the end of massless rod;

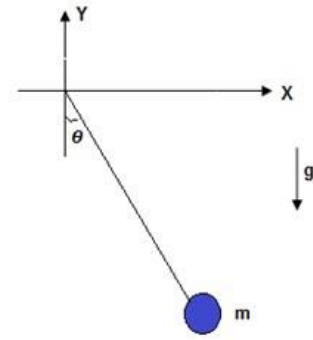
g = acceleration due to gravity;

b = damping constant;

θ = angular displacement of mass m from its equilibrium position;

$I = ml^2$, the moment of inertia of the system;

$\tau_{ext}(t)$ = external sinusoidal torque depending on time.



On the left of the above equation, the first term represents the resultant torque acting on the mass, second term is the damping force acting by air, third term is the gravitation force acting on the mass. On the right side, that is an external sinusoidal driving torque. The motion of the pendulum can be represented by angular displacement θ through time.

This equation belongs to nonlinear second order ordinary differential equation in which no analytical solution can be found. In addition, chaos appears in this system for certain conditions. Three different first-order ordinary differential equation can be separated from Eq(1) and that is the minimum number of dimensions that have the possibility of chaotic behaviors. This can be understood that if the phase space is in two dimensions, the trajectory cannot cross over itself, so the phase space plot is either periodic or spiral to a fixed point, and both are not chaotic. If one more dimension is added, the projection of the 3d phase space on 2d will have crossing trajectory and thus possibility of chaotic behaviors.

In this case, we make the variables as follows:

$$\omega = \frac{d\theta}{dt} \quad (2)$$

$$\phi = \omega_{ext} t \quad (3)$$

By substitution, we get the following sets of differential equations:

$$\frac{d\omega}{dt} + c\omega + \frac{g}{l}\sin\theta = F\sin(\omega_{ext}t) \quad (4)$$

$$\frac{d\theta}{dt} = \omega \quad (5)$$

$$\frac{d\phi}{dt} = \omega_{ext} \quad (6)$$

where the domain of θ is $(-\pi, \pi)$ and ϕ is $(0, 2\pi)$.

At lower θ , without damping and driving force, Eq(4) can be simplified into simple harmonic oscillator:

$$\frac{d^2\theta}{dt^2} = -\frac{g}{l}\theta \quad (7)$$

To solve the differential equation, we know that solution is in the form of sinusoidal function

$$\theta = A\cos(\omega t) + B\sin(\omega t) \quad (8)$$

By substitution and derivative of Eq(8), we can obtain $\omega_0^2 = \frac{g}{l}$ and $A = \theta_{t=0}$ and $B = \frac{\omega_{t=0}}{\omega_0}$, the analytical solution would then become the following equation:

$$\theta = \theta_{t=0}\cos(\omega t) + \frac{\omega_{t=0}}{\omega_0}\sin(\omega t) \quad (9)$$

where $\theta_{t=0}$ and $\omega_{t=0}$ are corresponding to angular displacement and velocity at $t=0$.

Algorithm designed

The program consists of three major parts: i) Arrays, discretized differential equations and variables initialization, ii) Implementation of numerical methods with error analysis, iii) Plot graph and animation for motion visualization.

The problem was analyzed and represented as set of first order ordinary differential equations Eq (4,5,6) in above section.

```
function [h_f, h_g] = motion_fn()
    [g,l,~,~,extF,extF_w,c,~,~,~] = get_var();    %%Get initial parameters
    h_f = @(time,theta,w) w;
    h_g = @(time,theta,w) -g/l*sin(theta) - c*w + extF*sin(extF_w*(time));
end
```

As the problem is an initial value problem, both Euler's method and forth order Runge-Kutta method were used in this project.

a) Euler's Method

For Euler's Method, we discretized the set of first order differential equations into the following:

$$\omega_{i+1} - \omega_i = h(-c\omega_i - \frac{g}{l}\sin\theta_i + F_{ext}\sin(\omega_{ext}t_i))$$

$$\theta_{i+1} - \theta_i = h\omega$$

```
function [time,theta,w] = euler_1(time,theta,w)
    [~,~,~,~,~,~,dt,~,duration] = get_var();
    [f,g] = motion_fn;
    % [f,g] = test_function_1;    %%For Function Test
    ind = 0:dt:duration;
    for i = 1:(length(ind)-1)
        %Two first order differential equations
        w(i+1) = w(i) + dt*g(time(i),theta(i),w(i));
        theta(i+1) = theta(i)+f(time(i),theta(i),w(i))*dt;
        time(i+1) = dt*i;
    end
end
```

As a result, we solve for the angular displacement and angular velocity as time evolves.

The global truncation error of Euler's approximation should be in order of h .

b) Forth order Runge-Kutta method (RK4)

Like Euler's method, the equation was discretized into the following equations using combinations of linear combinations of slope obtained in between the step size.

```
function [theta_new,w_new] = RK4_funcn(time,theta,w,dt)
    [f, g] = motion_fn;
    % [f,g] = test_function_1; %%For Function Test
    k1 = f(time, theta, w);
    l1 = g(time, theta, w);
    k2 = f(time+dt/2, theta+k1*dt/2, w+l1*dt/2);
    l2 = g(time+dt/2, theta+k1*dt/2, w+l1*dt/2);
    k3 = f(time+dt/2, theta+k2*dt/2, w+l2*dt/2);
    l3 = g(time+dt/2, theta+k2*dt/2, w+l2*dt/2);
    k4 = f(time+dt, theta+k3*dt, w+l3*dt);
    l4 = g(time+dt, theta+k3*dt, w+l3*dt);
    theta_new = theta + (k1 + 2*k2 + 2*k3 + k4)*dt/6;
    w_new = w + (l1 + 2*l2 + 2*l3 + l4)*dt/6;
end
```

```
function [time,theta,w] = RK4(time,theta,w)
    [~,~,~,~,~,~,dt,data_pts,duration] = get_var();
    ind = 0:dt:duration;
    error_1(1) = 0;
    for i = 1:(length(ind)-1)
        [theta(i+1),w(i+1)] = RK4_funcn(time(i),theta(i),w(i),dt);
        if i>1 %%For error analysis
            [theta_2h,w_2h] = RK4_funcn(time(i-1),theta(i-1),w(i-1),dt*2);
            abs_error_1(i) = theta_2h - theta(i+1);
            rel_error_1(i) = (theta_2h - theta(i+1)) / min(theta_2h, theta(i+1));
            if abs(abs_error_1(i)) > 1.e-3 || abs(rel_error_1(i)) > 1.e-3
                disp('Error too large');
                return
            end
        end
        time(i+1) = dt*i;
    end
    max(abs(abs_error_1)) %%For error analysis
    max(abs(rel_error_1)) %%For error analysis
    plot(error_1);
end
```

The global truncation error of RK4 approximation should be in order of h^4 .

As there is no exact analytical solution to the nonlinear second order ODEs, I have adjusted the step size by monitoring my estimated error from my algorithm. It was done by computing the local truncation absolute and relative error between θ approximation after two iteration with step size h and after one iteration with step size $2h$ throughout the whole iterations.

$$\theta_{i+2,h} - \theta_{i,h} = \frac{1}{6} 2h(k_1 + 2k_2 + 2k_3 + k_4)$$

The maximum absolute and relative error for all calculations in this work were controlled to be less than 1×10^{-10} and 1×10^{-5} respectively.

As the RK4 has better approximation as shown in later part of the report, it was used to simulate the pendulum motion instead of Euler's Method.

On the other hand, a higher order solver which is a built-in function "ode45" in MATLAB was used for comparison. The reason of choosing a higher order of solver is to validate my algorithm against a known solver and hoping that simulated results would not be meaningless. The absolute and relative error of my algorithm and ode45 were investigated.

For animation, it was done by plotting the solution of angular displacement for every specific time intervals. The frame of the figure was captured and using the MATLAB function "imwrite" to create a gif animation.

Results

The plane pendulum consists of a mass m hanging at the end of the massless rigid rod. It was restricted to move in plane. Acceleration of gravity g and length of massless rod to center of mass L were set to $9.8ms^{-2}$ and $9.8m$ respectively in all cases. Time started at $t = 0$, and angular velocity ω started at $0 rad s^{-1}$. External driving force and corresponding driving frequency will be denoted as F_{ext} and ω_{ext} respectively.

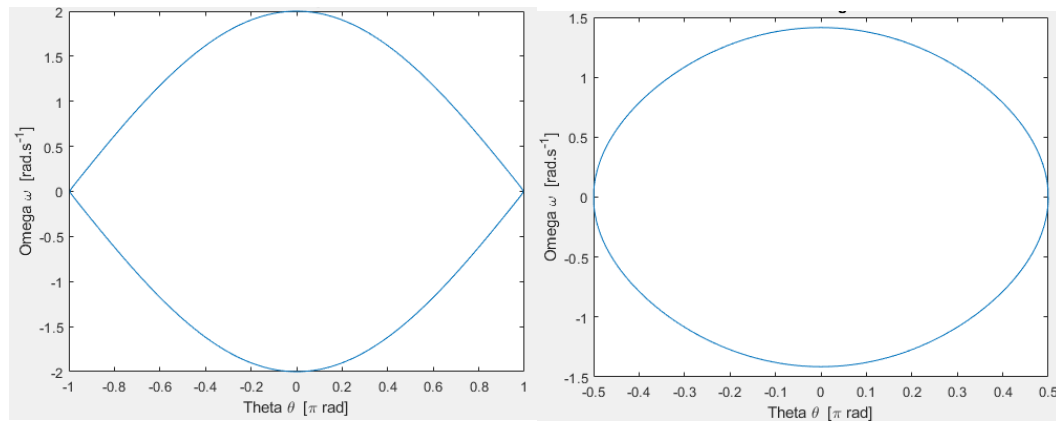


Fig. 1 Periodic phase space diagram for pendulum without driving and damping force for initial condition $\theta = 175^\circ$ (left) and $\theta = 90^\circ$ (right) after 200s.

State of driven pendulum can be described by θ, ω , and the phase difference between the driving torque and angular displacement. In this work, phase space was used to visualize the motion of pendulum. Phase space is defined as a space with orthogonal axis directions where the represented variables are required to specify the instantaneous state of the system. [5] It is defined by the above three quantities The trajectory in this phase space represent the motion of the pendulum and it is noted that the trajectory cannot cross over itself as the

future is unique from a given state. In our phase diagram, the trajectory can cross over each other because it is a projection from 3-dimensional phase space to 2 dimensional phase space (θ, ω) . This projection can show the concept of chaos effectively without too complicated plots and we can see that later on.

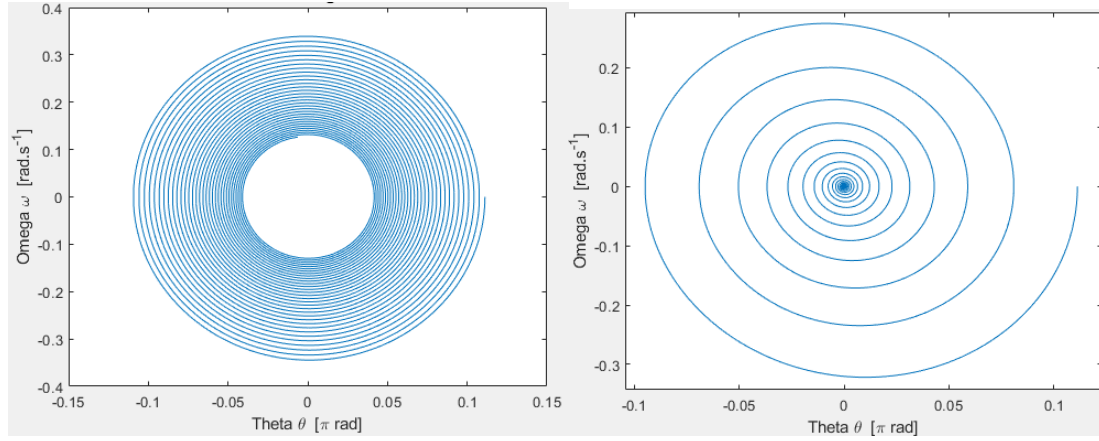


Fig. 2 Periodic phase space diagram for damped pendulum without driving force for with damping constant $c = 0.01$ (left) and $c = 0.1$ (right) after 200s.

For pendulum without damping and driving force, a closed curve can be observed in Fig. 1. That is expected as there is no damping force and driving torque. If damping force was added in top part of Fig. 2, we can observe a spiral towards a fixed point at origin, which is an attractor. Attractor can be defined as a set of numerical values in phase space that a system evolves along with time. [7] On the other hand, the attractor for an undamped pendulum with small angle is an ellipse which is a limit cycle. In top $\theta(t)$ plot of Fig. 3, we can observe the period $T = 2\pi\sqrt{\frac{l}{g}} = 2\pi$ s. In Fig From these phase space diagram, we can clearly observe the energy dynamics. The periodic phase space plot of pendulum loses no energy while the damped one does. The damping constant controls how fast system energy dissipates as we can see the amplitude of oscillation decreases eventually to zero.

Here we have several cases observing chaos behaviors. It is noted that the angular displacement was corrected to the unit of π rad.

CASE 1: Driven pendulum without damping

$w_{\text{ext}} = 1/3 \text{ rad s}^{-1}$ and $c = 0$ were kept constant while F_{ext} is the independent variable in Fig. (3,4).

As we increase the F_{ext} by 0.1 from 0 while holding all other variables constant, we can already observe changes in the whole motions Fig. (3). Although sign of period tripling occurs in phase space plot, the system still has certain periodic motion. As we increase the external driven force, the whole system starts to show chaos with weird aperiodic motion. The bottom right phase space curve clearly shows that the trajectory cross over itself so randomly but confined in a bounded space.

As we further increase the F_{ext} until $F_{\text{ext}} = 0.79$ in Fig. (4), the phase space is still bounded in $(-\pi, \pi)$. However, motion with $F_{\text{ext}}=0.7988$ has aperiodic motion with complete rotation. At this point, tiny variation on F_{ext} was tried, and the motion have complete rotations in completely different directions and the motion can never settle to a fixed point or limit cycle. These shows the extreme dependence on the initial conditions, which is a characteristic of chaotic dynamics.

CASE 2: Damped driven pendulum

$w_{\text{ext}} = 1/3 \text{ rad s}^{-1}$ and $c = 0.1$ were kept constant while F_{ext} is the independent variable in Fig. (5,6).

With damping, the motion of the pendulum without driving force converges to a fixed point while the pendulum with driving force converges to elliptic limit cycle for $F_{\text{ext}} = 0.1$ and wired shaped limit cycle for $F_{\text{ext}} = 0.5$ as shown in Fig. (5). That means the motion settles into a normal periodic oscillation for $F_{\text{ext}} = 0.1$ with frequency equal to the driving frequency ω_{ext} . For $F_{\text{ext}} = 0.5$, it can be observed that the angular displacement and velocity both have non-sinusoidal periodic pattern. As we increase the $F_{\text{ext}}=0.885$, the motion has complete rotations but eventually settle into a periodic motion as phase space plot shows that the motion tends to a limit cycle centered at $(\theta, \omega) = (-8\pi, 0)$ in Fig. 6. Little variation on F_{ext} to 0.886 shows chaotic aperiodic motion and does not settle to any fixed point or limit cycle within 200s.

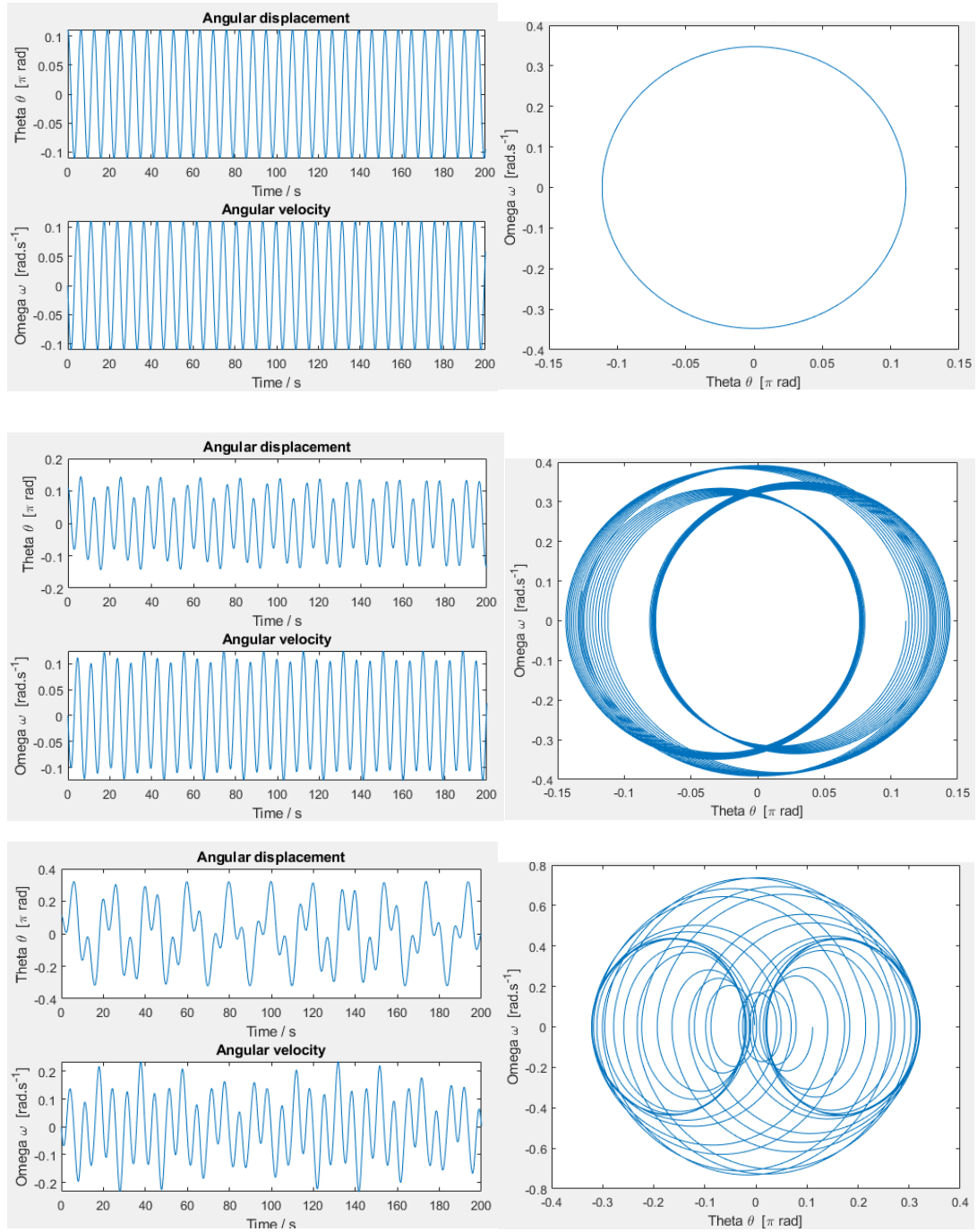


Fig. 3 Time evolution of θ , ω and phase space diagram for $F_{\text{ext}} = 0.0$ (Top), $F_{\text{ext}} = 0.1$ (Middle) and $F_{\text{ext}} = 0.5$ (Bottom) non-damped driven pendulum ($c = 0$, $w_{\text{ext}} = 1/3 \text{ rad s}^{-1}$). With a small variation of F_{ext} , phase diagram show that the motion of pendulum starts getting chaotic with increased F_{ext} .

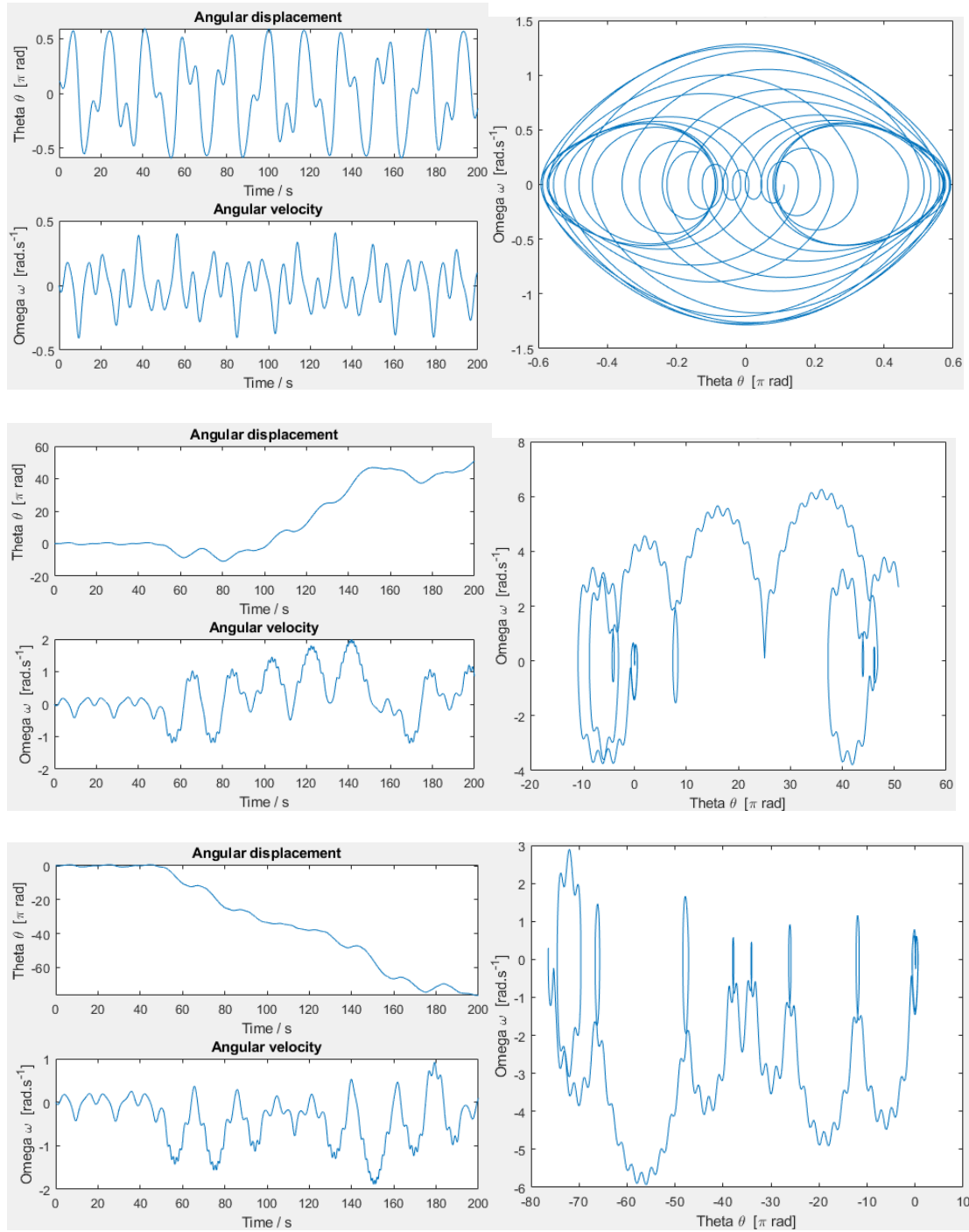


Fig. 4 Time evolution of θ, ω and phase space diagram for $F_{\text{ext}} = 0.79$ (Top), $F_{\text{ext}} = 0.7988$ (Middle) and $F_{\text{ext}} = 0.799$ (Bottom) non-damped driven pendulum ($c = 0$, $w_{\text{ext}} = 1/3 \text{ rad s}^{-1}$).

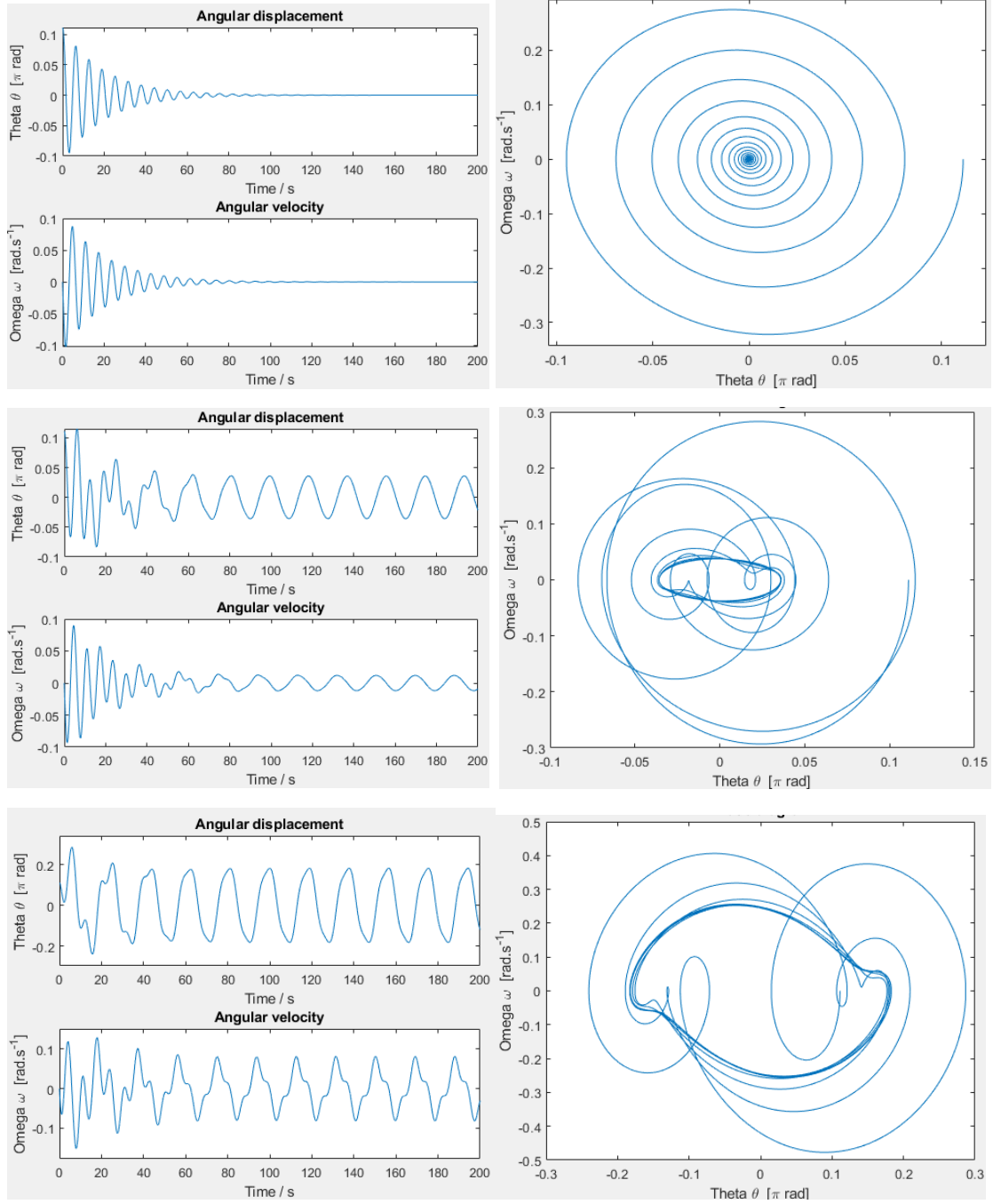


Fig. 5 Time evolution of θ , ω and phase space diagram for $F_{\text{ext}} = 0.0$ (Top), $F_{\text{ext}} = 0.1$ (Middle) and $F_{\text{ext}} = 0.5$ (Bottom) for damped driven pendulum ($c = 0.1$, $w_{\text{ext}} = 1/3 \text{ rad s}^{-1}$). With a small variation of F_{ext} , transition of chaotic damped oscillation to periodic oscillation can be seen.

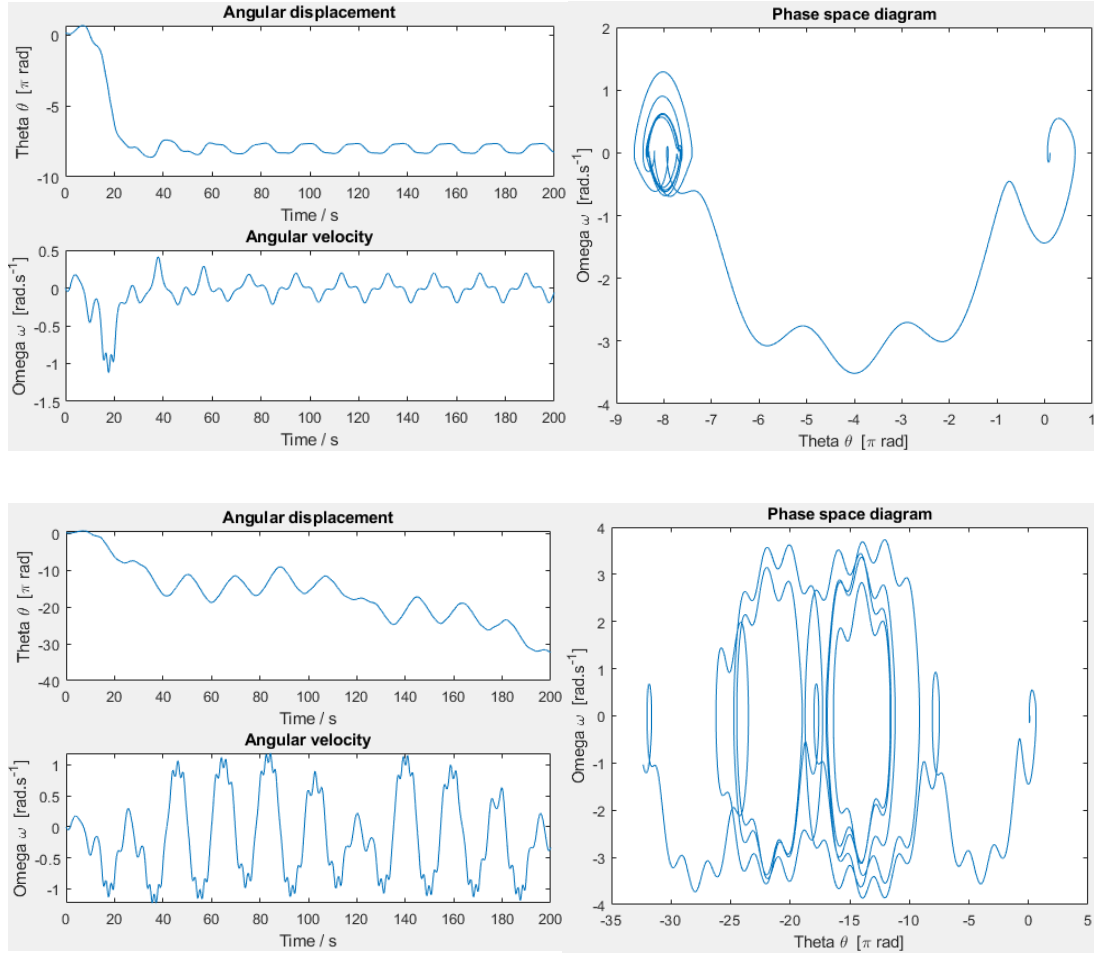


Fig. 6 Time evolution of θ, ω and phase space diagram for $F_{\text{ext}} = 0.885$ (Top), $F_{\text{ext}} = 0.886$ (Middle) for damped driven pendulum ($c = 0.1$, $w_{\text{ext}} = 1/3 \text{ rad s}^{-1}$).

CASE 3: F_{ext} were held constant for non-damped driven pendulum and the independent variable is ω_{ext} . Fig.(7)

Variation of driving frequencies was tried. Fig. (7) shows the double, triple and quadruple of period for the motion, which is $\frac{2\pi}{n\omega_{\text{ext}}} = 6.347$ where n is the period number of period multiplication. Period doubling and so on are defined as number of oscillations with different amplitudes occur before the pendulum return to the original state, e.g. period doubling means 2 oscillations with different amplitudes in one cycle. This feature can be observed in other chaotic dynamics.

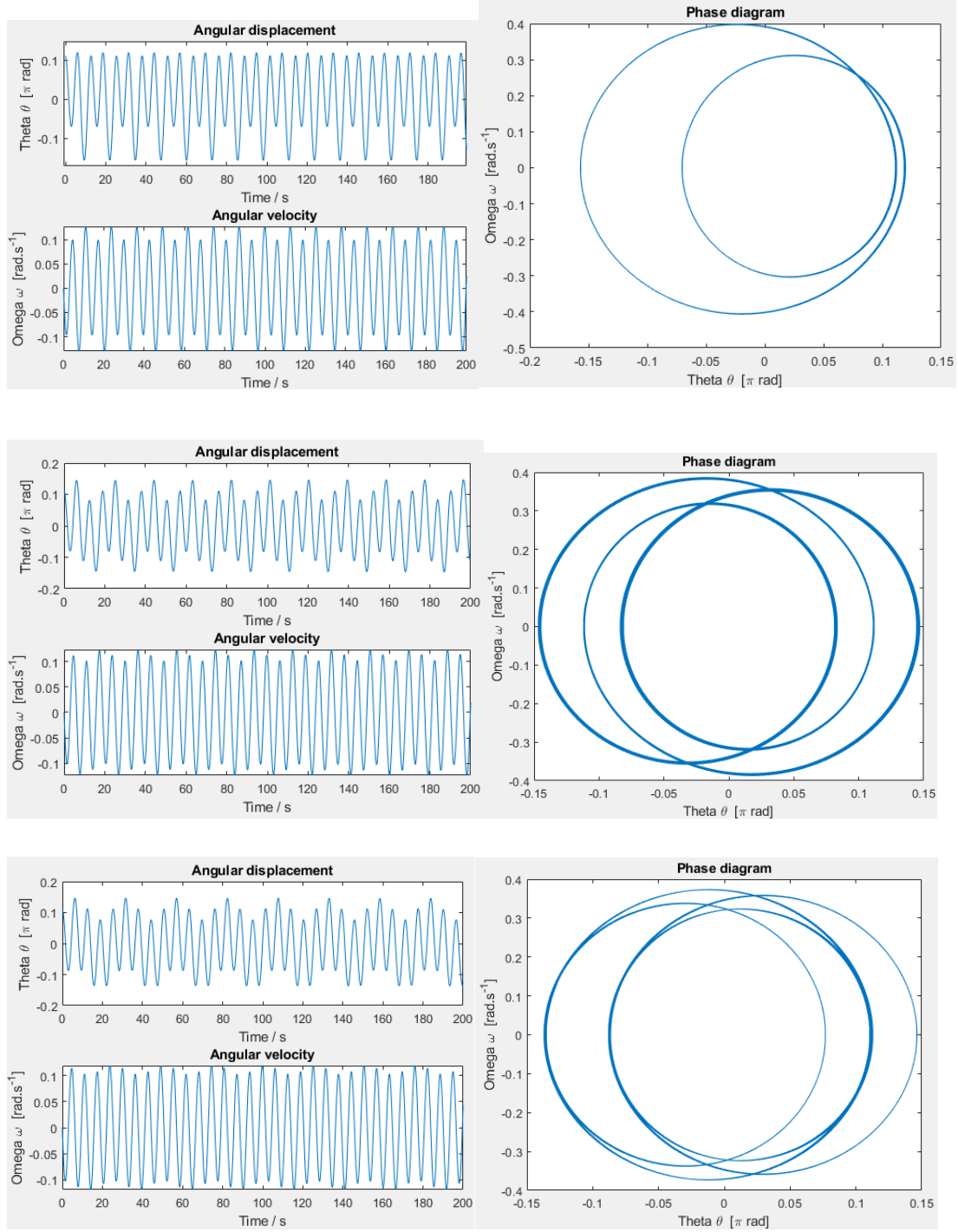


Fig. 7 Time evolution of θ, ω and phase space diagram for $\omega_{\text{ext}} = 0.495 \text{ rad s}^{-1}$ (Top), $\omega_{\text{ext}} = 0.33 \text{ rad s}^{-1}$ (Middle) and $\omega_{\text{ext}} = 0.248 \text{ rad s}^{-1}$ for non-damped driven pendulum ($c = 0$, $F_{\text{ext}} = 0.1$). With a small variation of ω_{ext} , the system has completely different behaviors. Top picture also shows sign of doubling period which often occurs in chaotic system.

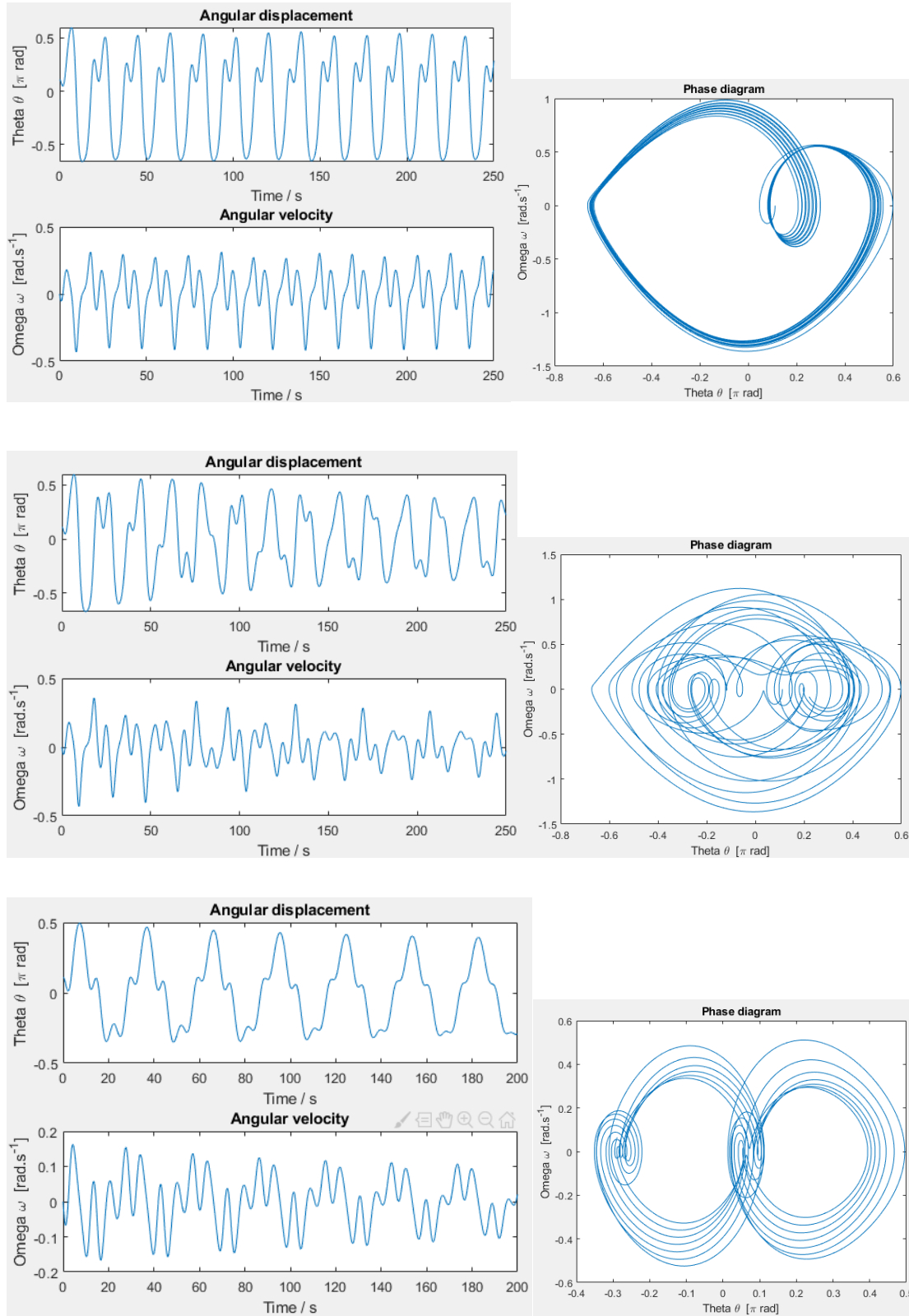


Fig. 8 Time evolution of θ, ω and phase space diagram for $\omega_{\text{ext}} = 1/3 \text{ rad s}^{-1}$ (Top), $\omega_{\text{ext}} = 0.334 \text{ rad s}^{-1}$ (Middle), $\omega_{\text{ext}} = 0.215 \text{ rad s}^{-1}$ (Bottom) for damped driven pendulum ($c = 0.01$, $F_{\text{ext}} = 0.81$). With a tiny variation of ω_{ext} between top and middle, the system has completely different behaviors. The system acquires order at one specific point later.

CASE 4: F_{ext} and damping coefficient was held constant and the independent variable is ω_{ext} .

Fig (8)

Variation of driving frequencies was tried. Top and bottom of Fig. (8) show the double quadruple of period for the motion. As shown in Fig. (8), the pendulum goes chaotic when driving frequency goes from $1/3 \text{ rad s}^{-1}$ to 0.334 rad s^{-1} with such a small variation. However, we can observe the dynamics has order with $\omega_{\text{ext}} = 0.215 \text{ rad s}^{-1}$. The energy of the system dissipates due to the damping coefficient so the space plot slowly spiral inside unlike the graphs in CASE 3. As the driving frequency increasing, the bifurcations come faster and eventually the period of oscillation will be infinite which is chaotic. [5]

Error analysis

When theta is small, the system can be approximated as a simple harmonic oscillation.

ITERATION	STEP SIZE	EULER	ABS. ERROR	RK4	ABS. ERROR
101	0.1	-4.090454359	1.596279634	-2.49417	3.146287670E-06
201	0.05	-3.19965216	0.705477436	-2.49417	1.428671460E-07
401	0.025	-2.825751259	0.331576534	-2.49417	7.242349000E-09
801	1.25E-02	-2.654927295	0.160752571	-2.49417	3.998548159E-10
1601	6.25E-03	-2.573323823	0.079149099	-2.49417	2.334310523E-11
3201	3.13E-03	-2.533446427	0.039271702	-2.49417	1.413980044E-12
6401	1.56E-03	-2.513735356	0.019560632	-2.49417	8.437694987E-14

Table 1 Absolute error comparison between Euler's and forth order Runge-Kutta methods solving set of first order linear ordinary differential equations of simple harmonic oscillator.

STEP SIZE	ABS. ERROR	ERROR/2	ABS. ERROR	ERROR/2 ⁴
0.1	1.596279634	0.798139817	3.146287670E-06	1.966429794E-07
0.05	0.705477436	0.352738718	1.428671460E-07	8.929196625E-09
0.025	0.331576534	0.165788267	7.242349000E-09	4.526468125E-10
0.0125	0.160752571	0.080376285	3.998548159E-10	2.499092600E-11
6.25E-03	0.079149099	0.039574549	2.334310523E-11	1.458944077E-12
3.13E-03	0.039271702	0.019635851	1.413980044E-12	8.837375276E-14
1.56E-03	0.019560632	0.009780316	8.437694987E-14	5.273559367E-15

Table 2 Relationship between step size (h) and the global truncation error accumulated after the whole simulation. As the step size halved, the error using Euler's method was also halved. On the other hand, the error using forth order Runge-Kutta methods was reduced by dividing 2⁴ indicating the error is on the order h^4 .

According to the analytical solution Eq. (9), true value of angular displacement $t=10$ is - 2.49417472448695 rad. Comparing the Euler's method and RK4, we can clearly see that the approximation of Euler's method has much larger error than RK4. RK4 has good approximation even when the step size is 0.1s.

As the step size halved, the absolute error by Euler's method is also halved which means the global truncation error is in the order of h . RK4 was roughly divided by 2⁴ when the step size halved indicating that the global truncation error is in the order of h^4 . These results agree with the order of error term calculated through Taylor's expansion.

In this work, I have monitored the local truncation absolute and relative error between θ approximation after two iterations with step size h and after one iteration with step size $2h$

throughout the all iterations. These maximum absolute and relative errors in this work were controlled to be less than 1×10^{-10} and 1×10^{-5} respectively.

On the other hand, the absolute and relative error between my fourth order Runge-Kutta method and built-in MATLAB solver “ode45” were also monitored after each simulation. Both errors are usually below 1×10^{-5} . However, it can be observed that the difference between ode45 and my RK4 varieties so much as shown in Fig. 8. With this initial condition, the system is completely chaotic. The error is majorly due to the chaotic behavior (very sensitive to the given state) of the system and any tiny uncertainty was magnified.

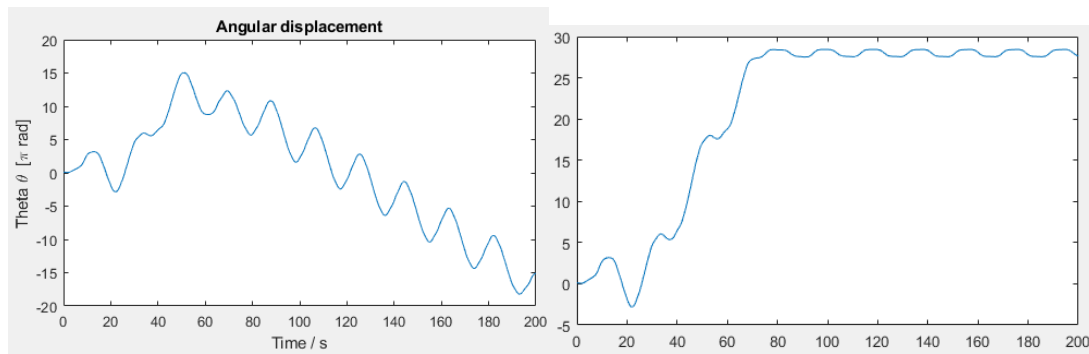


Fig. 8 Resulting angular displacement curve from my RK4 (left) and ode45 (right). $\theta = 20^\circ, \omega = 0, F_{ext} = 1, \omega_{ext} = \frac{1}{3}, c = 0.1, \text{step size} = 0.003125$ at $t = 0$.

Conclusion

In conclusion, the simulation of the second order differential equation was successfully carried out. The concept of system sensitivity to initial conditions was clearly captured which is a important feature of chaotic system. Variation of external driving torque or external driving frequency alone can lead to chaos. With the driving force, the system is always chaotic. Driven pendulum with damping will sometimes converge to periodic oscillation where phase space converges into limit cycle while driven pendulum without damping will not. With variation in driving frequency, period doubling can be observed which is a feature of chaotic system. In addition, animation for the motion was done for the ease of visualization. All in all, this simulation and phase space diagram definitely help us to understand the chaotic dynamics, and it is more than just investigating the pattern of angular displacement and velocity. This simulation is a good experience and definitely help us to understand more on both the numerical analysis and chaos theory on nonlinear dynamics.

References

1. R. Devaney et al., A First Course in Chaotic Systems, Perseus Books Publishing, 1992
2. S. H. Kellert et al., In the wake of chaos: unpredictable order in dynamical systems, the University of Chicago Press, Chicago. 1993
3. F. C. Hoppensteadt et al., Analysis and simulation of chaotic systems, Springer-Verlag, New York, 2000.
4. M. W. Hirsch et al., Differential Equations, Dynamical Systems, the University of Chicago Press, Chicago, 2004
5. G. L. Baker et al., Chaotic dynamics: an introduction, Cambridge Univ Pr, 1996.
6. Boeing, G. (2016). "Visual Analysis of Nonlinear Dynamical Systems: Chaos, Fractals, Self-Similarity and the Limits of Prediction". Systems. 4 (4): 37.
7. D.J. Bennett et al., Randomness. Harvard Univ Pr, 1999.